

Preparation of the Elusive [(por)Fe(NO)(O-ligand)] Complex by Diffusion of Nitric Oxide into a Crystal of the Precursor**

Nan Xu,* Lauren E. Goodrich, Nicolai Lehnert,* Douglas R. Powell, and George B. Richter-Addo*

Ferric heme proteins with nitric oxide (NO) as an axial ligand are critical components for the regulation of NO biosynthesis by the enzyme NO synthase,^[1] for NO transport (as vasodilator) in nitrophorins,^[2] for NO inhibition of cytochrome P450 and related enzymes,^[3] and these species have been identified as intermediates in cyt *cd*₁ dissimilatory nitrite reductases^[4] and in NO reduction by a fungal cyt P450 NO reductase.^[5] Ferric heme nitrosyls are generally described by the Fe^{II}-NO⁺ electronic ground state that is dominated by π backbonding, although the alternative low-spin Fe^{III}-NO electronic state is close in energy.^[6] The physiological functions of ferric nitrosyl heme proteins are clearly dependent on the character of their Fe-NO moieties. Thus, it is of great interest to investigate a range of ferric nitrosyl hemes that vary in *trans* axial ligand donor character (for example, S-, N-, and O-donors), as these *trans* ligands are expected to influence the electronics and hence functions of the Fe-NO groups. Previous investigations of the effect of axial *trans* ligands on ferric-NO groups have focused on thiolate systems, and a surprising *trans* effect of axial thiolate coordination was reported to influence both the geometry and electronics of the Fe-NO unit.^[7] Unfortunately, ferric nitrosyl hemes are much more difficult to isolate in pure form than their ferrous counterparts owing to the relatively weak binding of NO to ferric heme.^[8] This difficulty in the isolation and structural characterization of ferric heme nitrosyls has greatly hindered a complete analysis of the effects of NO binding to these ferric hemes.

Heme catalases^[9,10] and heme-binding HasAp proteins^[11] contain tyrosine as an axial ligand. The coordination of tyrosine to the heme plays a critical role for the functions that

these proteins carry out. It is known that the direct binding of NO to the iron center in heme catalases can result in reversible inhibition of enzyme activity,^[12] and the Cat^{III}(NO)^[13] and Cat^{II}(NO)^[14] compounds have been reported previously. However, only one protein crystal structure of a catalase-NO derivative has been reported; unfortunately, the low occupancy of NO (ca. 55%) and resolution of the structure prevented an accurate determination of the Fe-NO geometry (which could be modeled in the 175–160° range with weak restraints, and up to ca. 110° if no restraints were applied).^[15] Surprisingly, no neutral [(por)Fe(NO)(O-ligand)] model species has been characterized by spectroscopy or crystallography to model the active site of NO-inhibited heme catalase and related proteins. The closest examples are the structurally characterized [(TPP)Fe(NO)(H₂O)]ClO₄,^[16] [(TPP)Fe(NO)(H₂O)]-SO₃CF₃,^[17] and [(TPP)Fe(NO)(HO-*i*-C₅H₁₁)]ClO₄ species^[18] (H₂TPP = 5,10,15,20-tetraphenylporphyrin), but all three contain cationic iron nitrosyl porphyrin moieties. Herein, we utilize a heterogeneous crystal-gas method^[17,19,20] for the first preparation and accurate structural determination of a neutral [(por)Fe(NO)(O-ligand)] species, namely [(TPP)Fe(NO)(OC(=O)CF₃)] (2). We are thus now able to determine, for the first time, the *trans* effect of anionic O-based ligands on NO and compare our results across a range of ferric nitrosyl porphyrins with axial ligands of varied donor strength.

Dissolution of the five-coordinate compound [(TPP)Fe(OC(=O)CF₃)] (1) in CH₂Cl₂ reveals a band at 1715 cm⁻¹ in its IR spectrum assigned to ν_{CO} . Exposure of this solution to about 5 equiv of NO gas reveals a new strong band at 1907 cm⁻¹ assigned to the ν_{NO} of [(TPP)Fe(NO)(OC(=O)CF₃)] (2), as shown in Figure 1; the original ν_{CO} band at 1715 cm⁻¹ shifts to lower frequency.

This ν_{NO} value of 1907 cm⁻¹ is lower than those of the six-coordinate cations [(TPP)Fe(NO)(L)]⁺ (L = Lewis base; 1910–1925 cm⁻¹ in CH₂Cl₂) and is higher than those of the

[*] Dr. N. Xu, Dr. D. R. Powell, Dr. G. B. Richter-Addo
Department of Chemistry and Biochemistry, University of Oklahoma
101 Stephenson Parkway, Norman, OK 73019 (USA)
E-mail: xunan@ou.edu
grichteraddo@ou.edu
Homepage: <http://nitroso.ou.edu>

L. E. Goodrich, Dr. N. Lehnert
Department of Chemistry, University of Michigan
930 N. University, Ann Arbor, MI 48109 (USA)
E-mail: lehnertn@umich.edu

[**] This work was supported by a grant from the U.S. National Science Foundation (CHE-1213674 to G.B.R.-A. and CHE-0846235 to N.L.). The authors also acknowledge a grant from the NSF (grant CHE-0130835) and the University of Oklahoma for funds to purchase the X-ray instrument and computers.

Supporting information for this article is available on the WWW under <http://dx.doi.org/10.1002/ange.201208063>.

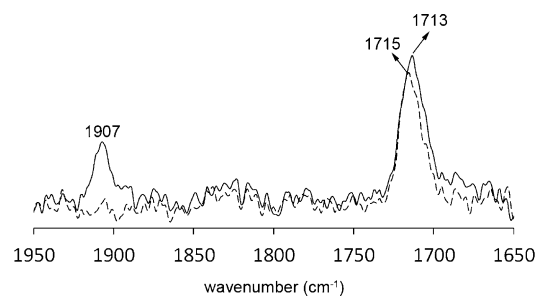


Figure 1. IR spectra recorded before (----) and after (—) the addition of NO gas to [(TPP)Fe(OC(=O)CF₃)] (1) in CH₂Cl₂.

neutral compounds [(TPP)Fe(NO)(halide)] (1889–1873 cm^{-1} ; CH_2Cl_2), [(TPP)Fe(NO)R] (R = alkyl, aryl; 1850–1764 cm^{-1} in Nujol), and [(OEP)Fe(NO)(SR)] (SR = thiolate; 1850 cm^{-1} in CH_2Cl_2).^[19,21]

The weak binding of NO in this ferric product **2** is evidenced by its complete dissociation (loss of ν_{NO}) when N_2 is bubbled into the product solution to restore the ν_{CO} band of the starting complex. Addition of a large excess of NO to the five-coordinate precursor [(TPP)Fe(OC(=O)CF₃)] results in the formation of [(TPP)Fe(NO)(OC(=O)CF₃)] as the predominant species initially, but the known byproducts [(TPP)Fe(NO)]⁺ (ν_{NO} 1844 cm^{-1}), [(TPP)Fe(NO)] (ν_{NO} 1681 cm^{-1}), and [(TPP)Fe(NO)(NO₂)] (ν_{NO} 1886 cm^{-1}) also form with time.^[22] Indeed, attempted crystallization of the product [(TPP)Fe(NO)(OC(=O)CF₃)] from solution resulted in the generation of this mixture of products, as the crystallization needed to be performed in the presence of excess NO.

We then turned to the crystal-gas method for trapping and X-ray crystal structural characterization of the target [(TPP)Fe(NO)(OC(=O)CF₃)] by diffusing NO gas into crystals of the five-coordinate precursor [(TPP)Fe(OC(=O)CF₃)].^[23–25] Crystals of **1** under an anaerobic atmosphere were exposed to NO at room temperature for 12 h. The IR spectrum of the product revealed the ν_{NO} band at 1901 cm^{-1} (KBr). The molecular structure of **2** is shown in Figure 2, and

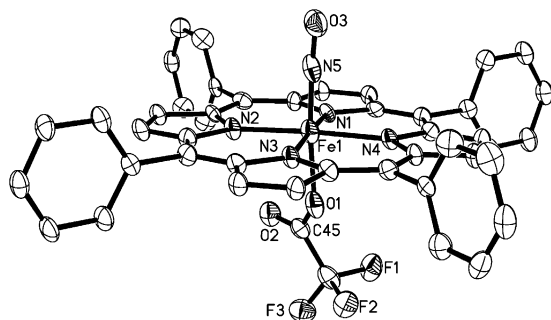


Figure 2. Molecular structure of [(TPP)Fe(NO)(OC(=O)CF₃)] (**2**), with ellipsoids set at 35% probability. Hydrogen atoms have been omitted for clarity.

selected structural data for **1** and **2** (for comparison) are collected in Table 1 (for the structure of the precursor **1**, see Supporting Information, Figure S1).

Several structural features of the product **2** are notable. First, the Fe–N–O moiety in the formally {FeNO}⁶ product **2** is almost linear with an angle of 175.8(6)°. Second, upon NO binding, the porphyrin macrocycle adopts a near-planar conformation in the six-coordinate product, in contrast to the saddled conformation observed in the five-coordinate precursor **1**.^[26] Next, the Fe atom in **2** displays a dramatic, circa 0.52 Å apical movement into the porphyrin plane from its initial position 0.45 Å towards the acetate ligand in the precursor.^[27,28] A shortening of the Fe–N_{por} bond lengths accompany this apical movement of the Fe atom in the crystal. Interestingly, the *trans* Fe–O bond in the product **2** is slightly shorter, by about 0.03 Å, than that found in the

Table 1: Selected structural data [Å, °] for compounds **1** and **2**.

	1	2
Fe1–N5		1.618(8)
N5–O3		1.151(8)
Fe1–N _{por}	2.048(2)–2.073(2)	2.004(6)–2.019(6)
Fe1–O1	1.932(2)	1.899(6)
Fe1–N5–O3		175.8(6)
O1–Fe1–N5		174.1(3)
C45–O1–Fe1	126.4(2)	132.7(5)
ΔFe ^[a]	0.45	0.07
O tilt ^[b]	3.5 [2.8]	1.7 [1.0]

[a] Apical displacement of the Fe atom from the 24-atom mean porphyrin plane towards the acetate ligand. [b] Tilt of the Fe-bonded acetate O atom from the normal to the porphyrin 4N [24-atom] plane.

precursor **1**. An accompanying opening of the Fe–O–C (acetate) angle, from 126° to 133°, occurs upon binding of the NO ligand (Table 1), reflecting the closer approach of the axial acetate ligand to the porphyrin macrocycle in the product. Finally, the mean-plane separation of adjacent face-to-face porphyrins increases from 4.4 Å in the precursor to 4.8 Å in **2**, and the lateral shift shows an incredible increase from 7.8 Å to 9.7 Å upon NO binding (Figure 3). This results

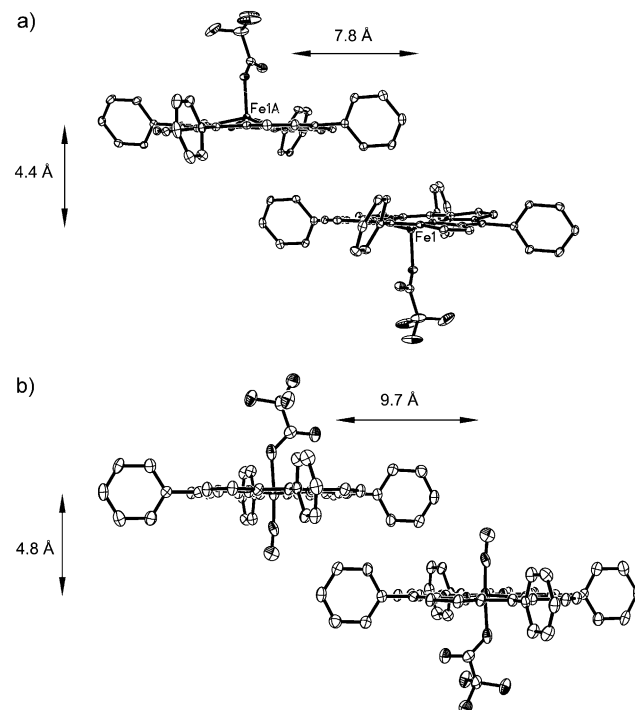


Figure 3. The packing diagram showing the relative positioning of two adjacent molecules in crystals of a) [(TPP)Fe(OC(=O)CF₃)] (**1**) and b) [(TPP)Fe(NO)(OC(=O)CF₃)] (**2**) with ellipsoids set at 35% probability.

in a net expansion of the unit cell from 2093.1(3) Å³ in the precursor **1** to 2144(3) Å³ in the product **2**, but without a significant loss in crystal quality.

To determine if the crystal lattice expansion that occurred upon NO diffusion into the crystal had any influence on the observed Fe–NO geometry (for example, whether the lattice expansion occurred because of steric hindrance involving the

newly formed Fe–NO groups), we performed density functional theory (DFT) calculations on the model compound [(porphine)Fe(NO)(OC(=O)CF₃)]. The BP86/TZVP optimized structure of this model compares well with the crystal structure of [(TPP)Fe(NO)(OC(=O)CF₃)]; the calculated Fe–N–O angle of 175.8° is identical to the experimentally determined angle (Supporting Information, Table S1). This indicates that the slight bending of the Fe–NO unit is an inherent electronic property of the complex and not a result of steric restraints imposed by packing of the crystal lattice. Key molecular orbitals for [(porphine)Fe(NO)(OC(=O)CF₃)] are shown in Figure 4 (charge contributions are listed in the

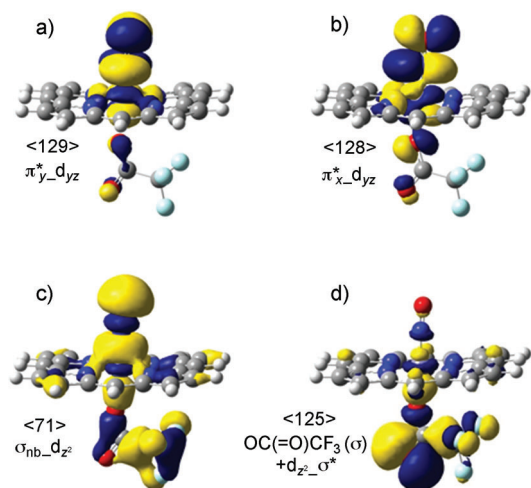


Figure 4. Important molecular orbitals of [(P)Fe(NO)(OC(=O)CF₃)] calculated with BP86/TZVP (P = porphine macrocycle). a) and b) correspond to the strong π backbonding interactions, c) to the weak σ interaction, and d) to the antibonding $\sigma^*_{d_z}$ -type interaction involved in the bending of the Fe–NO unit.

Supporting Information, Table S2). The main bonding interaction between the Fe center and the nitrosyl ligand in this low-spin compound (with Fe^{II}–NO⁺ character)^[6] corresponds to two strong π -backbonds from the d_{xz} and d_{yz} orbitals of Fe^{II} into the empty π^*_x and π^*_y orbitals of NO⁺, respectively (Figure 4a,b). The strength of the π -backbond is best estimated from the charge contributions of the corresponding antibonding combinations; for example, the MO (129) (that is, LUMO+1) has 28% d and 65% π^*_y character, which corresponds to a strong interaction. Additionally, a weak σ -bonding MO is observed at lower energy between the d_{z^2} (5%) orbital of Fe and the σ_{nb} (64%) orbital of NO (Figure 4c).

To better understand the electronic effect of the trifluoroacetate ligand on the Fe–NO geometry, we compared the geometry optimized structure of **2** with that of the non-fluorinated acetate complex [(porphine)Fe(NO)(OC(=O)CH₃)], where acetate is expected to be a stronger donor than trifluoroacetate. In the latter case, the Fe–N–O angle bends by 5° (compared with **2**), reflecting a stronger *trans* effect of the axial acetate ligand on the bound NO. Extension of this comparison to the ferric nitrosyls

[(porphine)Fe(NO)(MeIm)]⁺,^[6] [(porphine)Fe(NO)(NO₂)],^[29] and [(porphine)Fe(NO)(SPh)]^[7] reveals that the stronger the donation from the axial (anionic) ligand is, the weaker the Fe–NO and N–O bonds become (direct correlation), and the more the Fe–N–O units bend (Figure 5, Table 2; Supporting Information, Table S3). The calculated Fe–NO and N–O force constants and frequencies and Fe–N–O angles agree with this trend.

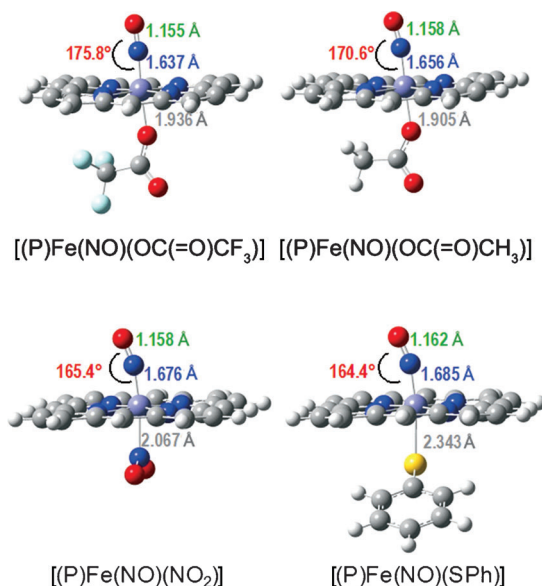


Figure 5. Optimized geometric parameters of [(P)Fe(NO)(X)] calculated with BP86/TZVP (P = porphine macrocycle).

Table 2: DFT calculated structural data (BP86/TZVP; [Å, °]) of representative ferric nitrosyl porphyrins.

	Fe–NO	Fe–N–O	Fe–X ^[a]
[(porphine)Fe(NO)(MeIm)] ⁺	1.644	180.0	2.018
[(porphine)Fe(NO)(OC(=O)CF ₃)]	1.637	175.8	1.936
[(porphine)Fe(NO)(OC(=O)CH ₃)]	1.656	170.6	1.905
[(porphine)Fe(NO)(NO ₂)]	1.676	165.4	2.067
[(porphine)Fe(NO)(SPh)]	1.685	164.4	2.343

[a] The distance between the Fe atom and the coordinating atom of the ligand *trans* to NO.

Importantly, the observed Fe–NO bending correlates with increased backbonding into a σ^* (a fully Fe–N–O antibonding) orbital of the Fe–NO unit (for example, Figure 4d), labeled $d_{z^2}\sigma^*$. This orbital is unoccupied in the Im complex, but becomes partially occupied by admixture into the occupied MO that results from the bonding interaction of the σ -donor orbital of the anionic ligand and d_{z^2} of iron (Figure 4d). The charge contributions for the $d_{z^2}\sigma^*$ orbitals are listed in the Supporting Information, Table S4, for the different complexes investigated here. As expected, the largest admixture of the $d_{z^2}\sigma^*$ orbital is observed (15% Fe(d) and 4% NO(σ^*)) for the thiolate complex having the strongest axial donor and correspondingly, the most bent Fe–N–O angle. Hence, as

demonstrated here for the first time, this backbond into the σ^* orbital of the Fe–NO unit is responsible for the weakening of the Fe–NO and N–O bonds, and the bending of the Fe–N–O unit, over a wide range of axial anionic ligand donor strengths. The observed bending of the Fe–N–O unit causes a small reduction of the unfavorable antibonding interaction between the d_{z^2} orbital of iron and the σ^* orbital of the formally NO^+ ligand, and in this way, leads to a small energy gain of the system.^[7]

In summary, we have successfully prepared the first member of the elusive class of neutral [(por)Fe(NO)(O-ligand)] compounds by employing a rare solid–gas two-phase reaction. The O-coordinated complex complements the known stable N-bonded and S-bonded derivatives. The molecular structure of this ferric nitrosyl does not reveal a lengthening of the *trans* iron–ligand bond as normally observed for the more common ferrous nitrosyl porphyrins with N-base ligands.^[30] The observed heme flattening upon NO binding is remarkable and, combined with our earlier observation in a cationic derivative,^[17] suggests that this feature may be more common than previously thought. It is interesting to note that such heme flattening upon binding NO has been suggested to play a significant role in the activation of the H-NOX family of sensor proteins that includes the mammalian enzyme soluble guanylyl cyclase responsible for blood pressure control.^[31] Our DFT computational results and analyses have provided an explanation of the variation in electronic structure and weakening of the Fe–NO/N–O bonds and the bending of the Fe–NO units in a range of ferric heme nitrosyls with varied axial ligand (O-, N-, S-) donor strengths. Based on these results, it is reasonable to suggest that the varied *trans* effects of axial ligands in ferric heme proteins play significant roles in determining the physiological functions of the Fe–NO moieties. We speculate, based on the weak binding of NO in our model ferric [(por)Fe(NO)(O-ligand)] complex and combined with our DFT results, that the O-coordinated tyrosine ligand in heme catalase is critical for preventing the irreversible inhibition of enzyme activity by NO.

Experimental Section

The five-coordinate compound [(TPP)Fe(OC(=O)CF₃)] was synthesized from the reaction of the oxo-dimer [(TPP)Fe₂(μ -O)] with trifluoroacetic acid, as described previously.^[25] Triclinic crystals of [(TPP)Fe(OC(=O)CF₃)] were grown from a 2:1 mixture of CH₂Cl₂/cyclohexane at room temperature.

Crystal data for **1** (C₄₆H₂₈F₃FeN₄O₂·(C₆H₁₂) (M_r = 865.73), triclinic, space group $P\bar{1}$, $a = 11.2285(9)$, $b = 12.0522(9)$, $c = 17.1643(13)$ Å, $\alpha = 72.885(2)$, $\beta = 82.233(2)$, $\gamma = 70.680(2)^\circ$, $V = 2093.1(3)$ Å³, $Z, Z' = 2$, $T = 100(2)$ K, $R1 = 0.0524$ ($I > 2\sigma(I)$), $wR2$ (all data) = 0.1407. Crystal data for **2** (C₄₆H₂₈F₃FeN₅O₃·(C₆H₁₂) (M_r = 895.74), triclinic, space group $P\bar{1}$, $a = 11.055(9)$, $b = 13.204(10)$, $c = 16.953(13)$, $\alpha = 85.074(9)$, $\beta = 72.130(9)$, $\gamma = 65.693(8)^\circ$, $V = 2144(3)$ Å³, $Z, Z' = 2, 1$, $T = 100(2)$ K, $R1 = 0.0812$ ($I > 2\sigma(I)$), $wR2$ (all data) = 0.2494. CCDC 904064 (**1**) and 904063 (**2**) contain the supplementary crystallographic data for this paper. These data can be obtained free of charge from The Cambridge Crystallographic Data Centre via www.ccdc.cam.ac.uk/data_request/cif.

DFT calculations (geometries and frequencies) were performed using Gaussian03 with the BP86 functional and TZVP basis set. Molecular orbitals were obtained from subsequent single-point calculations using ORCA. Details of the DFT calculations (such as geometries, frequencies, charge contributions to important MOs, force constants) are given in the Supporting Information.

The synthesis and crystallography were performed at the University of Oklahoma, and the DFT calculations were performed at the University of Michigan.

Received: October 7, 2012

Revised: January 12, 2013

Published online: March 4, 2013

Keywords: iron · nitrogen oxides · porphyrinoids · structure elucidation · X-ray diffraction

- [1] J. Santolini, S. Adak, C. M. L. Curran, D. J. Stuehr, *J. Biol. Chem.* **2001**, 276, 1233–1243.
- [2] F. A. Walker, *J. Inorg. Biochem.* **2005**, 99, 216–236.
- [3] D. A. Wink, Y. Osawa, J. F. Darbyshire, C. R. Jones, S. C. Eshenaur, R. W. Nims, *Arch. Biochem. Biophys.* **1993**, 300, 115–123.
- [4] B. A. Averill, *Chem. Rev.* **1996**, 96, 2951–2964.
- [5] A. Daiber, H. Shoun, V. Ullrich, *J. Inorg. Biochem.* **2005**, 99, 185–193.
- [6] V. K. K. Praneeth, F. Paulat, T. C. Berto, S. D. George, C. Nather, C. D. Sulok, N. Lehnert, *J. Am. Chem. Soc.* **2008**, 130, 15288–15303.
- [7] F. Paulat, N. Lehnert, *Inorg. Chem.* **2007**, 46, 1547–1549.
- [8] M. D. Lim, I. M. Lorkovic, P. C. Ford, *J. Inorg. Biochem.* **2005**, 99, 151–165.
- [9] C. D. Putnam, A. S. Arvai, Y. Bourne, J. A. Tainer, *J. Mol. Biol.* **2000**, 296, 295–309.
- [10] M. K. Safo, F. N. Musayev, S.-H. Wu, D. J. Abraham, T.-P. Ko, *Acta Crystallogr. Sect. D* **2001**, 57, 1–7.
- [11] G. Jekporir, J. C. Rodriguez, H. A. Rui, W. Im, S. Lovell, K. P. Battaile, A. Y. Alontaga, E. T. Yukl, P. Moenne-Loccoz, M. Rivera, *J. Am. Chem. Soc.* **2010**, 132, 9857–9872.
- [12] G. C. Brown, *Eur. J. Biochem.* **1995**, 232, 188–191.
- [13] M. Hoshino, K. Ozawa, H. Seki, P. C. Ford, *J. Am. Chem. Soc.* **1993**, 115, 9568–9575.
- [14] P. Nicholls, *Biochem. J.* **1964**, 90, 331–343.
- [15] N. Purwar, J. M. McGarry, J. Kostera, A. A. Pacheco, M. Schmidt, *Biochemistry* **2011**, 50, 4491–4503.
- [16] W. R. Scheidt, Y. J. Lee, K. Hatano, *J. Am. Chem. Soc.* **1984**, 106, 3191–3198.
- [17] N. Xu, D. R. Powell, G. B. Richter-Addo, *Angew. Chem.* **2011**, 123, 9868–9870; *Angew. Chem. Int. Ed.* **2011**, 50, 9694–9696.
- [18] G.-B. Yi, L. Chen, M. A. Khan, G. B. Richter-Addo, *Inorg. Chem.* **1997**, 36, 3876–3885.
- [19] N. Xu, D. R. Powell, L. Cheng, G. B. Richter-Addo, *Chem. Commun.* **2006**, 2030–2032.
- [20] This method bypasses the traditional crystallization process from solution, which frequently results in decomposition of ferric nitrosyl porphyrins.
- [21] “Binding and Activation of Nitric Oxide by Heme and Metalloporphyrins”: L. Cheng, G. B. Richter-Addo, in *The Porphyrin Handbook*, Vol. 4 (Eds.: R. Guilard, K. Smith, K. M. Kadish), Academic Press, New York, **2000**, chap. 33, pp. 219–291.
- [22] Dissolution of a powdered heterogeneous mixture of [(TPP)Fe(OC(=O)CF₃)] and [(TPP)Fe(solvent)₂][OC(=O)CF₃] in CH₂Cl₂ followed by exposure to NO results in the formation of [(TPP)Fe(NO)(OC(=O)CF₃)] and [(TPP)Fe(NO)][OC(=O)CF₃].

- [23] The compound has been crystallized previously in the monoclinic $P2_1/a$ form.^[24]
- [24] S. A. Moy, J. A. Gonzalez, L. J. Wilson, *Acta Crystallogr. Sect. C* **1995**, *51*, 1490–1494.
- [25] Complex **1** and other five-coordinate iron porphyrin carboxylates are high-spin: H. Oumous, C. Lecomte, J. Protas, P. Cocolios, R. Guillard, *Polyhedron* **1984**, *3*, 651–659.
- [26] A similar porphyrin flattening upon NO binding to a five-coordinate iron porphyrin has been reported.^[17]
- [27] The observation of out-of-plane Fe atoms in five-coordinate iron porphyrins and essentially in-plane Fe atoms in six-coordinate iron nitrosyl porphyrins has been analyzed previously.^[28]
- [28] G. R. A. Wyllie, W. R. Scheidt, *Chem. Rev.* **2002**, *102*, 1067–1089.
- [29] I. V. Novozhilova, P. Coppens, J. Lee, G. B. Richter-Addo, K. A. Bagley, *J. Am. Chem. Soc.* **2006**, *128*, 2093–2104.
- [30] G. R. A. Wyllie, C. E. Schultz, W. R. Scheidt, *Inorg. Chem.* **2003**, *42*, 5722–5734.
- [31] S. Muralidharan, E. M. Boon, *J. Am. Chem. Soc.* **2012**, *134*, 2044–2046.
-